NASA Technical Memorandum 100202

Detailed Mechanism of Benzene Oxidation

(NASA-TM-100202) DETAILED MECHANISM OF BENZENE OXIDATION (NASA) 24 p Avail: NTIS HC A03/MF A01 CSCL 07D

N88-11775

Unclas
G3/25 0107320

David A. Bittker
Lewis Research Center
Cleveland, Ohio

October 1987

NASA

ERRATA

NASA Technical Memorandum 100202

DETAILED MECHANISM OF BENZENE OXIDATION

by David A. Bittker

October 1987

Page 4, at the bottom of the page, add the following lines:

Other C-H-O Reactions

Two reactions which play a significant role in generating radicals that control the benzene ignition process are reactions 3 and 9. The rate constants for these H_2-O_2-CO system reactions are well established and are taken from

Page 16, Table II, reaction number 14: The species C_6H_6OH should be C_6H_5OH

Page 17, Table III, reaction number 14: The species C_6H_6OH should be C_6H_5OH

DETAILED MECHANISM OF BENZENE OXIDATION

David A. Bittker
National Aeronautics and Space Administration
Lewis Research Center
Cleveland, Ohio 44135

E-3797

SUMMARY

A detailed benzene oxidation mechanism, which uses the qualitative paths outlined by previous investigators, is presented. Ignition delay times for argon-diluted mixtures computed with this mechanism are in satisfactory agreement with experimental values obtained from pressure-time profiles for a wide range of initial conditions. An experimental temperature versus time profile measured in a nitrogen diluted mixture has also been successfully computed. Additional computations have qualitatively matched several experimental species concentration versus time profiles for the nitrogen diluted reaction. Application of sensitivity analysis allowed the approximate determination of the rate constants for two important reactions:

$$C_6H_5 + O_2 \overset{k_7}{\rightleftharpoons} C_6H_5O + O$$

$$k_7 = 4.5\times10^{12}\ e^{-15000\ cal/RT}\ cm^3\ mol^{-1}s^{-1}$$

and

$$C_5H_5 + O_2 \overset{k_{10}}{\rightleftharpoons} C_5H_5O + O$$

$$k_{10} = 2.0\times10^{12}\ e^{-20000\ cal/RT}\ cm^3\ mol^{-1}s^{-1}$$

INTRODUCTION

The increasing importance of aromatics in the practical hydrocarbon fuels of today has accelerated research aimed at improving our understanding of the high-temperature oxidation of these compounds. This knowledge is important in controlling the combustion and emission characteristics of both advanced aircraft propulsion and future ground-based gas turbines. The oxidation and pyrolysis of the simplest aromatic, benzene, have been studied by several investigators (refs. 1 to 4). A recent review paper (ref. 5) on aromatic hydrocarbon oxidation presents experimentally measured temperature and composition profiles for oxidation of one benzene-oxygen-nitrogen mixture in a highly turbulent flow reactor. In some recent work (ref. 6) ignition delay time measurements were reported for benzene-oxygen-argon mixtures ignited behind a reflected shock. The experimental conditions covered a wide range of initial composition, temperature, and pressure. The ignition delay times were determined from pressure versus time profiles.

The purpose of the present paper is to develop a detailed mechanism which reproduces the results of references 5 and 6 over the widest possible range of initial conditions. Computations were performed with the new NASA Lewis general chemical kinetics and sensitivity analysis code (refs. 7 to 9). To achieve the best possible agreement sensitivity analysis was used to identify the most important reactions. Adjustments were then made to some of the reaction rate constants in the mechanism. However, only rate constants with large uncertainties were changed significantly. These adjustments were made mainly to reactions involving benzene and its fragments. The rate constants for reactions involving other hydrocarbons, e.g., acetylene and methane, were used at their literature values. In the sections which follow, we present comparisons of computed and experimental results and discuss the mechanism finally obtained for optimal matching with the latter results. We also describe the sensitivity study which determined the reactions which have the greatest effect on the computed results.

BENZENE OXIDATION MECHANISM

We have followed the general scheme outlined qualitatively in references 1 and 5. The oxidation process can be divided into three stages:

Initiation: The formation of oxygen and hydrogen atoms and OH radicals as well as some phenyl radicals by the pyrolysis of benzene and its reaction with molecular oxygen.

Induction: Rapid formation of phenyl radical and its oxidation and pyrolysis to form primarily phenoxy radical, C_6H_5O; further reaction of C_6H_5O to form phenol, cyclopentadiene, and acetylene.

Combustion: Oxidation of the stable intermediate hydrocarbons and radical recombinations which cause the main heat release.

In the initiation region the following reactions were assumed:

$$C_6H_6 + O_2 \overset{k_1}{\rightleftharpoons} C_6H_5 + HO_2 \tag{1}$$

$$C_6H_6 \overset{k_2}{\rightleftharpoons} C_6H_5 + H \tag{2}$$

$$H + O_2 \overset{k_3}{\rightleftharpoons} OH + O \tag{3}$$

In the induction region the reactions used were as follows:

$$H + C_6H_6 \overset{k_4}{\rightleftharpoons} C_6H_5 + H_2 \tag{4}$$

$$O + C_6H_6 \overset{k_5}{\rightleftharpoons} C_6H_5 + OH \tag{5}$$

$$OH + C_6H_6 \overset{k_6}{\rightleftharpoons} C_6H_5 + H_2O \quad (6)$$

We have written reactions 4 through 6 as simple abstraction processes, although the possibility of addition processes has been suggested (ref. 5).

$$C_6H_5 + O_2 \overset{k_7}{\rightleftharpoons} C_6H_5O + O \quad (7)$$

$$C_6H_5O + M \overset{k_8}{\rightleftharpoons} C_5H_5 + CO + M \quad (8)$$

cyclo-
pentadienyl

$$CO + OH \overset{k_9}{\rightleftharpoons} CO_2 + H \quad (9)$$

$$C_5H_5 + O_2 \overset{k_{10}}{\rightleftharpoons} C_5H_5O + O \quad (10)$$

$$C_5H_5O + M \overset{k_{11}}{\rightleftharpoons} C_4H_5 + CO + M \quad (11)$$

butadienyl

$$C_6H_5OH \overset{k_{12}}{\rightleftharpoons} C_6H_5O + H \quad (12)$$

$$C_5H_5 + C_6H_6 \overset{k_{13}}{\rightleftharpoons} C_5H_6 + C_6H_5 \quad (13)$$

cyclo-
pentadiene

$$OH + C_6H_5OH \overset{k_{14}}{\rightleftharpoons} C_6H_5O + H_2O \quad (14)$$

$$C_6H_5 \overset{k_{15}}{\rightleftharpoons} C_4H_3 + C_2H_2 \quad (15)$$

$$M + C_4H_3 \overset{k_{16}}{\rightleftharpoons} C_4H_2 + H + M \quad (16)$$

$$C_5H_6 + O + \overset{k_{17}}{\rightleftharpoons} C_5H_5O + H \quad (17)$$

$$C_4H_5 \overset{k_{18}}{\rightleftharpoons} C_2H_3 + C_2H_2 \quad (18)$$

These are the significant steps which occur in the initiation and induction regions. Additional reactions, discussed later, are needed to model the combustion region and determine the concentrations of intermediate species. The

complete set of reactions is necessary for modeling the temperature and composition profiles.

REACTION RATE CONSTANTS

In this section we discuss the selection of rate constants for those reactions involving benzene and its decomposition products which have been studied in recent experimental work. Sources for rate constant of combustion-zone reactions are also given.

Benzene Pyrolysis Reaction

The pyrolysis of benzene has been studied recently in two investigations, by Hsu, Lin, and Lin (Ref. 4) and by Kiefer et al. (Ref. 10). This work has shown that reaction (2) is the only important path at high temperature. The pyrolysis rate constant was measured as a function of temperature and pressure. For the temperature and pressure range of the present computations we have used the expression given in reference 4, which agrees well with results of reference 10.

Radical Attacks on Benzene

Reactions 4, 5 and 6 are the main reactions for generating phenyl radical. We have used the rate constant of reference 10 for the $H + C_6H_6$ reaction. The recently reported experimental values of references 11 and 12 were used for the $O + C_6H_6$ and $OH + C_6H_6$ reactions. In a later section we discuss sensitivity analysis computations which showed the pressure and temperature profiles to be quite insensitive to moderate variations of these three rate constants from their literature values. This is true, even though these reactions are all important sources of phenyl radical.

Other C_6 and C_5 Reactions

The rate constants of some reactions of phenyl and phenoxy (C_6H_5O) radical have been measured recently. The previously quoted work of reference 10 has determined rate constant expressions for the phenyl radical pyrolysis, reaction 15. Their high-pressure unimolecular reaction expression was used in the present computations. The estimated rate constant for pyrolysis of C_4H_3, reaction 16, is also taken from reference 10. The rate constant for the phenoxy pyrolysis, reaction 8, is the value of Lin and Lin (ref. 13). The rate constants for other reactions in the induction region had to be either estimated or adjusted to match the experimental data. The sensitivity analysis computations for accomplishing this task are described below.

reference 14. The reactions of acetylene, which are important in the combustion region, were all taken from reference 15. The complete mechanism consisted of 110 reactions among 35 species. All reactions and rate constants used for these computations are given in table I.

SENSITIVITY ANALYSIS STUDY

To identify the important reactions which control the oxidation of benzene and its fragments in the induction zone, an extensive sensitivity analysis was performed. Normalized sensitivity coefficients were computed using the decoupled direct method described in references 8 and 9. These coefficients give the variation of all species concentrations, temperature and pressure with changes in the individual rate constant parameters A_j, n_j, and E_j of the modified Arrhenius equation $k_j = A_j T^{n_j} \exp(-E_j/RT)$ for reaction j. In the present work sensitivity coefficients of several species concentrations plus temperature and pressure with respect to the A_j parameters were used to determine the important reactions. Table II shows these coefficients for the nitrogen diluted stoichiometric oxidation of benzene (initial temperature = 1115 K) in the turbulent flow reactor described in reference 5. The reaction is at constant pressure so no pressure sensitivity coefficient is given. The results show that the reactions of C_6H_5 and C_5H_5 radicals with molecular oxygen have greatest effect on temperature and several species composition profiles. Table III shows sensitivity coefficients for a typical stoichiometric benzene oxygen-argon shock ignition (initial temperature = 1405 K) from reference 6. Sensitivity coefficients of pressure are now included. Again the dominant reactions are the C_6H_5 and C_5H_5 oxidations. Computations were also performed for a second shock ignition at equivalence ratio = 2 and an initial temperature of 1600 K. Sensitivity coefficients for four dependent variables and five reactions are shown for both conditions in table IV for ease of comparison. The data in table IV show that computed results should be most sensitive to the rate constant of reaction 7, the phenyl oxidation, at both conditions. However, there is a significant change in the sensitivity coefficients for reaction 15, the phenyl pyrolysis. These coefficients change from very small values for the stoichiometric lower temperature reaction to much larger values for the rich higher temperature reaction. The effect of reaction 15 on the pressure profile is now indicated to be greater than that of reaction 10.

The predictions of the sensitivity coefficients were tested by using the "brute force" or indirect method of sensitivity analysis. The preexponential factor for each reaction in table IV was changed by factors of 2 and 0.5 and the ignition computation was repeated for each change. The effect of these rate constant variations on the computed pressure profile is shown in table V. Given in this table are values of τ_p, the ignition-delay time measured from the pressure versus time profile as described in detail in the next section. For each reaction we show the τ_p values for k_{std}, the rate constant listed in table I, and also τ_p for $2k_{std}$ and $k_{std}/2$. Also shown are the percent changes in τ_p for each rate constant variation. the computed results in table V confirm all the sensitivity predictions of table IV. In particular, changing k_{15} for the lower-temperature stoichiometric mixture has a very small effect on τ_p. The same change in k_{15} has a very significant effect on τ_p for the high-temperature rich mixture.

The results of these sensitivity computations were used in the following way to adjust the rate constant parameters. The A_j and E_j values for reactions 7 and 10 were adjusted in several iterations to give the best match to the ignition delay times of reference 6 and the temperature versus time profile of reference 5 for the benzene-oxygen-nitrogen reaction. It was found, from the matching of ignition delay times, that the activation energy of the dominant reaction 7 should be as high as possible. This reaction is an exothermic process and we have used the upper limit, suggested in reference 1, of 15 kcal/mole. The C_5H_5 oxidation, reaction 10, is about 10 kcal/mole endothermic at 1200 K. An activation energy of 20 kcal/mole was found to give the best shape to the computed temperature versus time profile for the benzene-oxygen-nitrogen reaction. The prexponential factors of both these reactions were then adjusted to give the best match to both the ignition-delay times and the temperature versus time profile. Table V and the sensitivity coefficients of table II show that reaction 7 strongly controls the τ_p computation and that reactions 7 and 10 both have important effects on the temperature versus time profile. Therefore the prexponential factor A_7 was determined by matching the ignition-delay times and A_{10} was then adjusted to give the best match to the temperature versus time profile. The values obtained are:

$$k_7 = 4.5 \times 10^{12}\ e^{-15000\ cal/RT}\ cm^3\ mol^{-1}s^{-1}$$

$$k_{10} = 2.0 \times 10^{12}\ e^{-20000\ cal/RT}\ cm^3\ mol^{-1}s^{-1}$$

Other rate constants for reactions involving cyclopentadiene, phenol and their fragments were estimated and adjusted to give the best agreement with reported experimental phenol and cyclopentadiene profiles in reference 5.

DESCRIPTION OF COMPUTATIONAL PROCEDURE

In this section we describe briefly the apparatus and experimental procedures reported in references 5 and 6. We then describe our mathematical model used to simulate each of these reacting systems.

Turbulent Flow Reactor

Temperature and composition versus time profiles for the reaction of a stoichiometric benzene-oxygen mixture in a nitrogen atmosphere were obtained in the Princeton University flow reactor (ref. 5). A detailed description of this turbulent, chemical-rate limited device is given in reference 16. The reactants were highly diluted in nitrogen to eliminate diffusion effects. Profiles of temperature and composition with respect to distance were converted to time profiles by taking into account the flow velocities within the reactor. The exact zero of reaction time is arbitrary and was taken as point of fuel injection into the hot oxidant stream. Reference 16 indicates that the reactor is operated at one atmosphere pressure. In the computations, therefore, the flow reactor was modeled as a constant pressure homogeneous batch reaction. For all kinetic computations of this work, the thermodynamic data are from the NASA Lewis Research Center data base which is part of the NASA Chemical Equilibrium Composition Computer code of Gordon and McBride (ref. 22). The recently reported data of Burcat, Zeleznik and McBride (ref. 23) were used for phenyl and phenoxy radicals. New thermodynamic data for several benzene pyrolysis and

oxidation fragments (C_4H_3, C_4H_5, C_5H_5 and C_5H_5O) were estimated by Bonnie J. McBride. Computed time profiles of temperature and several species concentrations were compared to the profiles presented in reference 5.

Shock-Tube Ignition Experiments

The ignition delay times of Ref. 6 were obtained from measured pressure versus time traces following ignition behind a reflected shock wave. The time interval between ignition and the first observed "significant" pressure rise was taken as the ignition delay time, τ. To match the experimental technique as closely as possible the computed ignition delay time, τ_p, was obtained from the computed pressure versus time curve. The kinetic computations were performed assuming a constant-volume batch reaction behind the reflected shock. Before performing the kinetic computations the initial reflected shock conditions in reference 6 were recomputed. A small correction for attenuation of the reflected shock velocity was applied to each data point. The reflected shock initial tempertures and pressures (T_5 and p_5) were then recomputed using the Chemical Equilibrium Code of reference 22. Complete time profiles of temperature, pressure, and all species concentrations were then computed. A typical computed pressure versus time curve is shown in figure 1. Also shown is the method used to determine the τ_p value by the intersection of two extrapolated lines. This method approximated as closely as possible the experimental technique. Only 35 of the experimental points reported in reference 6 were used for our comparisons. The other points were excluded from consideration for one of two different reasons. First, all points for which τ was less than 100 μsec were excluded. These values are inaccurate because of pressure disturbances which propagate in the shock tube and cause nonuniform heating of the gas behind the reflected shock. Details of this effect are given in reference 19. Second, all the data taken for the experimental mixture with equivalence ratio of 0.25 were excluded because it was very difficult to determine accurate τ values from these pressure traces. The pressure rise was very poorly defined for all these very weak ignitions.

Table VI lists the five mixtures from reference 6 which were used in the present comparisons along with the initial temperature range of the reflected shocks. Mixtures 3 and 4 are identical for all practical purposes and are treated as one condition, equivalence ratio 1.0 with about 85 percent argon dilution. Note that comparison of the results for mixture 2 with those for mixtures 3 and 4 gives the effect of simply diluting the mixture with argon at a constant equivalence ratio. Initial pressures for the reflected shocks ranged from 1.7 to 7.1 atm.

RESULTS AND DISCUSSION

Comparison of Computed and Experimental Ignition Delay Times

Plots of computed and experimental ignition delay time versus reciprocal of temperature are shown in figures 2 to 6 for the four different initial conditions given in table VI. The individual computed and experimental points are shown as well as least-squares lines for each set of points. They are fitted to the empirical equation

$$\tau = Ae^{\Delta E/RT} \tag{1}$$

or

$$\log \tau = \log A + \frac{\Delta E}{2.303\ RT} \tag{2}$$

where R is the universal gas constant and ΔE is an activation energy term which measures the temperature dependence of τ for a fixed set of initial concentrations. A detailed comparison of experimental and computed results is shown in table VII, which also includes an error analysis. The percent difference between each computed and experimental value is given along with the percent standard deviation for each set of initial concentrations used. This standard deviation is defined by

$$\sigma = \sqrt{\frac{\sum_{i=1}^{N}\left(\frac{\tau_{ex} - \tau_p}{\tau_{ex}}\right)^2}{N}} \times 100\ \% \tag{3}$$

where N is the number of points. A value of σ for all 35 points used is also given.

Examination of this table shows satisfactory agreement between the computed and experimental ignition delays. This is especially true when one considers the uncertainty in some of the experimental measurements. For example, table VII shows three instances in which the experimental results do not show the expected decrease of ignition delay time with increasing temperature. The agreement between experiment and computation is poorest for the lean mixture ($\phi = 0.5$) and steadily improves as ϕ increases to 2.0. Similar behavior is also observed for the temperature dependence of ignition delay. This can be seen from table VIII which lists the values of ΔE computed from equation (1) for both the experimental and computed results. The percent deviation for the activation energies decreases steadily as equivalence ratio changes from 0.5 to 2.0. From these comparisons it appears that one or more reactions are missing from the mechanism. These reactions are much more important in the lean mixtures than in the rich ones. However, it should also be pointed out that the experimental ignition delay times for the lean mixtures are more uncertain than those for the rich mixtures. From figures 2 and 5 it can be seen that the computations tend to overpredict the ignition delay time at $\phi = 0.5$ and underpredict it at $\phi = 2.0$.

Figure 6 shows computed and experimental ignition delay plots for two mixtures with equivalence ratio of 1.0 but with different amounts of argon diluent. The computed results show a much smaller effect of inert dilution than observed experimentally. The effect of inert gas dilution could not be changed by variation of either the A factor or the activation energy of any uncertain rate constants.

Comparison of Computed and Experimental Temperature and Composition Profiles

Figures 7 to 12 show computed temperature versus time and several composition versus time profiles along with experimental data for the nitrogen-diluted stoichiometric C_6H_6-O_2 reaction reported in reference 5. The initial mixture temperature was 1115 K and the pressure was 1 atmosphere. The computed and experimental temperature profiles in figure 7 are in excellent quantitative agreement. The computed cyclopentadiene profile of figure 8 is in semiquantitative agreement with the experimental profile. Both the peak concentration of C_5H_6 and the time at which it is reached are predicted quite accurately. The computed profiles for phenol (fig. 9) benzene (fig. 10) and carbon monoxide (fig. 11) agree only with the qualitative trends of the corresponding experimental profiles. For phenol, the computation matches the magnitude on the peak concentration, but this value occurs at a later reaction time. The mechanism predicts a very sudden disappearance of benzene, instead of the gradual decay observed experimentally. The experimental rise of carbon monoxide concentration and its peak value are greater than the corresponding computed quantities. There is semi-quantiative agreement between the computed and experimental carbon dioxide profiles (fig. 12). The computed profile is approximately linear whereas the experimental profile shows a long induction period. However, the same steady-state value found experimentally is given by the computed profiles.

An acetylene versus time profile is also given in reference 5 for this benzene oxidation experiment. The predicted acetylene peak concentration is about one order of magnitude lower than the reported experimental value. The sensitivity coefficients of table II show that this concentration is controlled by reactions 7 and 10, as are many other concentrations. No reasonable changes in any of the reactions involving acetylene changed its profile significantly. This behavior is different from that for cyclopentadiene and phenol. Although these latter two concentrations are also strongly controlled by reactions 7 and 10, they were significantly improved by modest adjustments of the rate constants for reactions 12 and 13, which are quite uncertain.

CONCLUDING REMARKS

This work has presented a detailed quantitative mechanism for the oxidation of benzene. The mechanism satisfactorily computes experimental results for both argon and nitrogen diluted systems. Fair to good agreement was obtained between computed and experimental ignition delay times measured over a wide range of temperature, pressure and composition for shock-heated benzene-oxygen-argon mixtures. The mechanism also does a fair job of computing measured temperature and composition profiles for a nitrogen-diluted benzene oxidation in a quite different system, namely a turbulent flow reactor.

The present work has verified the reaction paths outlined in references 1 and 5 and presents rate constant expressions for two important reactions. Sensitivity analysis has identified these reactions, the oxidations of C_6H_5 and C_5H_5 radicals, as being dominant in the ignition of benzene-oxygen mixtures. The expressions for these reaction rate constants have to be considered approximate because the mechanism is still incomplete. However, the mechanism predicted one temperature versus time profile accurately, in addition to the satisfactory ignition delay time predictions. Therefore, it could be used for heat-release rate predictions in practical, well-mixed, benzene-air combustion systems.

REFERENCES

1. Venkat, C.; Brezinsky, K.; and Glassman, I.: High Temperature Oxidation of Aromatic Hydrocarbons. Nineteenth Symposium (International) on Combustion, The Combustion Institute, Pittsburgh, 1983, pp. 143-152.

2. McLain, A.G.; Jachimowski, C.J.; and Wilson, C.H.: Chemical Kinetic Modeling of Benzene and Toluene Oxidation Behind Shock Waves. NASA TP-1472, 1979.

3. Kern, R.D., et al.: Collaborative Shock Tube Studies of Benzene Pyrolysis. Twentieth Symposium (International) on Combustion, The Combustion Institute, Pittsburgh, 1985, pp. 789-797.

4. Hsu, D.S.Y.; Lin, C.Y.; and Lin, M.C.: CO Formation in Early Stage High Temperature Benzene Oxidation Under Fuel Lean Conditions. Kinetics of the Initiation Reaction, $C_6H_6 \rightarrow C_6H_5 + H$. Twentieth Symposium (International) on Combustion, The Combution Institute, Pittsburgh, 1985, pp. 623-630.

5. Brezinsky, K.: The High Temperature Oxidation of Aromatic Hydrocarbons. Prog. Energy Combust. Sci., vol. 12, no. 1, 1986, pp. 1-24.

6. Burcat, A.; Snyder, C.; and Brabbs, T.A.: Ignition Delay Times of Benzene and Toluene with Oxygen in Argon Mixtures. NASA TM-87312, 1986.

7. Radhakrishnan, K.; and Bittker, D.A.: GCKP86-An Efficient Code for General Chemical Kinetics and Sensitivity Analysis Computations. Presented at the Eastern States Combustion Institute Meeting, Dec. 15-17, 1986.

8. Radhakrishnan, K.: Decoupled Direct Method for Sensitivity Analysis in Combustion Kinetics, NASA CR-179636, 1987.
Also in, Advances in Computer Methods for Partial Differential Equations VI, R. Vichnevetsky and R.D. Stepleman, eds., IMACs, 1987.

9. Radhakrishnan, K.; and Bittker, D.A.: GCKP87-An Efficient General Chemical Kinetics and Sensitivity Analysis Code for Gas-Phase Reactions. NASA TP-, 1987, (In preparation.)

10. Kiefer, J.H., et al.: Shock Tube Investigation of Major Pathways in the High-Temperature Pyrolysis of Benzene. J. Phys. Chem., vol. 89, no. 10, May 9, 1985, pp. 2013-2019.

11. Nicovich, J.M.; Gump, C.A.; and Ravishankara, A.R.: Rates of Reaction of $O(^3P)$ with Benzene and Toluene. J. Phys. Chem., vol. 86, no. 9, Apr. 29, 1982, pp. 1684-1690.

12. Madronich, S.; and Felder, W.: Kinetics and Mechanism of the Reaction of OH with C_6H_6 Over 790-1410 K, J. Phys. Chem., vol. 89, no. 16, Aug. 1, 1985, pp. 3556-3561.

13. Lin, C.-Y.; and Lin, M.C.: Thermal Decomposition of Methyl Phenyl Ether in Shock Waves: The Kinetics of Phenoxy Radical Reactions. J. Phys. Chem., vol. 90, no.3, Jan. 30, 1985, pp. 425-431.

14. Brabbs, T.A.; Belles, F.E.; and Brokaw, R.S.: Shock Tube Measurements of Specific Reaction Rates in the Branched-Chain H_2-CO-O_2 System. Thirteenth Symposium (International) on Combustion, The Combustion Institute, Pittsburgh, 1973, pp. 129-136.

15. Miller, J.A., et al.: Toward a Comprehensive Kinetic Mechanism for the Oxidation of Acetylene: Comparison of Model Predictions with Results From Flame and Shock Tube Experiments. Nineteenth Symposium (International) on Combustion, The Combustion Institute, Pittsburgh, 1983, pp. 181-196.

16. Hautman, D.J.: Pyrolysis and Oxidation Kinetic Mechanisms for Propane. PhD Thesis, Princeton University, 1980.

17. Westley, F.: Table of Recommended Rate Constants for Chemical Reactions Occurring in Combustion. NSRDS-NBS-67, Apr. 1980.

18. Westbrook, C.K.; and Dryer, F.L.: Chemical Kinetic Modeling of Hydrocarbon Combustion. Prog. Energy Combust. Sci., vol. 10, no. 1, 1984, pp. 1-57.

19. Brabbs, T.A.; and Robertson, T.F.: Methane Oxidation Behind Reflected Shock Waves: Ignition Delay Times Measured by Pressure and Flame Band Emission. NASA TM-87268, 1986.

20. Brabbs, T.A.; and Brokaw, R.S.: Shock Tube Measurements of Specific Reaction Rates in the Branched Chain CH_4-CO-O_2 System: Fifteenth Symposium (International) on Combustion, The Combustion Institute, Pittsburgh, 1975, pp. 893-901.

21. Cherian, M.A., et al.: Kinetic Modelling of the Oxidation of Carbon Monoxide in Flames. Eighteenth Symposium (International) on Combustion, The Combustion Institute, Pittsburgh, 1981, pp. 385-396.

22. Gordon, S.; and McBride, B.J.: Computer Program for Calculation of Complex Chemical Equilibrium Compositions, Rocket Performance, Incident and Reflected Shocks, and Chapman-Jouget Detonations, NASA SP-273, 1971.

23. Burcat, A.; Zeleznik, F.J.; and McBride, B.J.: Ideal Gas Thermodynamic Properties for the Phenyl, Phenoxy, and O-Biphenyl Radicals. NASA TM-83800, 1985.

TABLE I. - BENZENE OXIDATION MECHANISM

No.	Reaction	A cm^3, mole,sec	n	Ea calories per mole	Source
1	$C_6H_6 + O_2 = C_6H_5 + HO_2$	6.31×10^{13}	0	60 000	Ref. 2
2	$C_6H_6 = C_6H_5 + H$	5.0×10^{15}	0	108 000	Ref. 4
3	$H + O_2 = OH + O$	1.26×10^{14}	0	16 300	Ref. 14
4	$C_6H_6 + H = C_6H_5 + H_2$	2.5×10^{14}	0	16 000	Ref. 10
5	$C_6H_6 + O = C_6H_5 + OH$	2.78×10^{13}	0	4 910	Ref. 11
6	$C_6H_6 + OH = C_6H_5 + H_2O$	2.13×10^{13}	0	4 580	Ref. 12
7	$C_6H_5 + O_2 = C_6H_5O + O$	4.5×10^{12}	0	15 000	This work
8	$C_6H_5O = C_5H_5 + CO$	2.5×10^{11}	0	43 900	Ref. 13
9	$CO + OH = CO_2 + H$	4.17×10^{11}	0	1 000	Ref. 14
10	$C_5H_5 + O_2 = C_5H_5O + O$	2.0×10^{12}	0	20 000	This work
11	$C_5H_5O + M = C_4H_5 + CO + M$	7.59×10^{13}	0	15 000	Est.
12	$C_6H_5OH = C_6H_5O + H$	6.0×10^{13}	0	88 000	Est.
13	$C_5H_5 + C_6H_6 = C_5H_6 + C_6H_5$	2.0×10^{11}	0	10 000	Est.
14	$OH + C_6H_5OH = C_6H_5O + H_2O$	8.0×10^{12}	0	5 000	Est.
15	$C_6H_5 = C_4H_3 + C_2H_2$	1.58×10^{15}	0	82 000	Ref. 10
16	$M + C_4H_3 = C_4H_2 + H + M$	3.3×10^{51}	-10	63 000	Ref. 10
17	$C_5H_6 + O = C_5H_5O + H$	5.0×10^{12}	0	10 000	Est.
18	$C_4H_5 = C_2H_3 + C_2H_2$	1.4×10^{13}	0	32 900	Est.
19	$C_4H_2 + O = C_2HO + C_2H$	1.0×10^{13}	0	0	Ref. 2
20	$C_4H_2 + O = CO + C_3H_2$	1.2×10^{12}	0	0	Ref. 15

TABLE I. - Continued.

No.	Reaction	A cm^3, mole,sec	n	Ea calories	Source
21	$C_4H_2 + OH + HCO + C_3H_2$	$3.0x10^{13}$	0	0	Ref. 15
22	$C_2H_4 + M + C_2H_2 + H_2 + M$	$9.33x10^{16}$	0	77 200	Ref. 15
23	$C_2H_4 + OH = C_2H_3 + H_2O$	$4.79x10^{12}$	0	1 230	Ref. 18
24	$C_2H_4 + OH + CH_3 + CH_2O$	$2.00x10^{12}$	0	960	
25	$C_2H_4 + O + CH_3 + HCO$	$3.31x10^{12}$	0	1 130	
26	$C_2H_4 + O = CH_2O + CH_2$	$2.51x10^{13}$	0	5 000	
27	$C_2H_3 + M = C_2H_2 + H + M$	$7.94x10^{14}$	0	31 500	
28	$C_2H_3 + O_2 = C_2H_2 + HO_2$	$1.58x10^{13}$	0	10 000	Ref. 15
29	$C_2H_3 + H = C_2H_2 + H_2$	$6.0x10^{12}$	0	0	
30	$C_2H_3 + OH = C_2H_2 + H_2O$	$5.00x10^{12}$	0	0	
31	$C_2H_3 + CH_2 = C_2H_2 + CH_3$	$3.00x10^{13}$	0	0	
32	$C_2H_3 + C_2H = C_2H_2 + C_2H_2$	$3.00x10^{13}$	0	0	
33	$C_2H_3 + O = C_2H_2O + H$	$3.30x10^{13}$	0	0	
34	$CH_2 + CH_2 = C_2H_2 + H_2$	$4.00x10^{13}$	0	0	
35	$CH_2 + CH_2 = C_2H_3 + H$	$5.01x10^{12}$	0	0	Ref. 18
36	$CH_2 + OH = CH + H_2O$	$2.51x10^{11}$	.67	25 700	Ref. 15
37	$CH_2 + O = CH + OH$	$2.00x10^{11}$	.68	25 000	
38	$CH_2 + O_2 = CO_2 + 2H$	$1.59x10^{12}$	0	1 000	
39	$C_2H_2 + M = C_2H + H + M$	$4.17x10^{16}$	0	107 000	
40	$C_2H_2 + C_2H_2 = C_4H_3 + H$	$2.00x10^{12}$	0	45 900	
41	$C_2H_2 + O_2 = C_2HO + OH$	$2.00x10^{8}$	1.5	30 100	
42	$C_2H_2 + O = C_2H + OH$	$3.16x10^{15}$	-.6	15 000	
43	$C_2H_2 + O = CH_2 + CO$	$2.20x10^{10}$	1.0	2 580	
44	$C_2H_2 + O = C_2HO + H$	$3.55x10^{4}$	2.7	1 390	
45	$C_2H_2 + OH = C_2H + H_2O$	$6.31x10^{12}$	0	7 000	Ref. 18

TABLE I. - Continued.

No.	Reaction	A cm^3, mole,sec	n	Ea calories	Source
46	$C_2H_2 + OH = C_2H_2O + H$	3.20×10^{11}	0	200	Ref. 15
47	$C_2H_2 + C_2H = C_4H_2 + H$	3.00×10^{13}	0	0	
48	$C_2H_2 + CH_2 = C_3H_3 + H$	1.00×10^{12}	0	0	
49	$C_3H_3 + H + M = C_3H_4 + M$	2.00×10^{13}	0	0	
50	$C_2H_2O + OH = CH_2O + HCO$	2.80×10^{13}	0	0	
51	$C_2H_2O + OH = C_2HO + H_2O$	7.5×10^{12}	0	3 000	
52	$C_2H_2O + H = CH_3 + CO$	1.13×10^{13}	0	3 428	Ref. 18
53	$C_2H_2O + H = C_2HO + H_2$	7.50×10^{13}	0	8 000	Ref. 15
54	$C_2H_2O + O = C_2HO + OH$	5.00×10^{13}	0	8 000	
55	$C_2H_2O + O = CH_2O + CO$	2.00×10^{13}	0	0	
56	$C_2H_2O + M = CH_2 + CO + M$	2.00×10^{16}	0	60 000	
57	$C_2HO + O_2 = 2CO + OH$	1.46×10^{12}	0	2 500	
58	$C_2HO + O = 2CO + H$	1.20×10^{12}	0	0	Ref. 18
59	$C_2HO + OH = 2HCO$	1.00×10^{13}	0	0	Ref. 15
60	$C_2HO + H = CH_2 + CO$	5.00×10^{13}	0	0	
61	$C_2HO + CH_2 = C_2H_3 + CO$	3.00×10^{13}	0	0	
62	$C_2HO + CH_2 = CH_2O + C_2H$	1.00×10^{13}	0	2 000	
63	$C_2HO + C_2HO = C_2H_2 + 2CO$	1.00×10^{13}	0	0	
64	$C_2H + OH = C_2HO + H$	2.00×10^{13}	0	0	
65	$C_2H + O_2 = C_2HO + O$	5.00×10^{13}	0	1 500	
66	$C_2H + O = CO + CH$	5.00×10^{13}	0	0	
67	$C_2H + H_2 = C_2H_2 + H$	4.09×10^{6}	2.39	864	
68	$CH_4 + M = CH_3 + H + M$	2.00×10^{17}	0	88 000	Ref. 18
69	$CH_4 + O_2 = CH_3 + HO_2$	7.94×10^{13}	0	56 000	Ref. 18
70	$CH_4 + H = CH_3 + H_2$	1.26×10^{14}	0	11 900	Ref. 20

TABLE I. - Continued.

No.	Reaction	A cm^3, mole,sec	n	Ea calories	Source
71	$CH_4 + OH = CH_3 + H_2O$	$2.5x10^{13}$	0	5 010	Ref. 19
72	$CH_4 + O = CH_3 + OH$	$1.9x10^{14}$	0	11 720	Ref. 19
73	$CH_3 + OH = CH_2O + H_2$	$3.98x10^{12}$	0	0	Ref. 17
74	$CH_3 + OH = CH_3O + H$	$2.00x10^{16}$	0	27 410	
75	$CH_3 + O_2 = CH_3O + O$	$4.79x10^{13}$	0	29 000	
76	$CH_3 + O = CH_2O + H$	$1.29x10^{14}$	0	2 000	
77	$CH_3 + CH_3 = C_2H_4 + H_2$	$1.00x10^{16}$	0	32 000	
78	$CH_3O + M = CH_2O + H + M$	$5.01x10^{13}$	0	21 000	
79	$CH_3O + O_2 = CH_2O + HO_2$	$1.00x10^{12}$	0	6 000	
80	$CH_3O + H = CH_2O + H_2$	$2.00x10^{13}$	0	0	
81	$CH_3 + CH_2O = CH_4 + HCO$	$1.00x10^{10}$	.5	6 000	
82	$CH_3 + HCO = CH_4 + CO$	$3.02x10^{11}$	.5	0	
83	$CH_3 + HO_2 = CH_3O + OH$	$2.00x10^{13}$	0	0	
84	$CH_2O + M = HCO + H + M$	$3.31x10^{16}$	0	81 000	
85	$CH_2O + OH = HCO + H_2O$	$7.59x10^{12}$	0	170	
86	$CH_2O + H = HCO + H_2$	$3.31x10^{14}$	0	10 500	
87	$CH_2O + O = HCO + OH$	$5.01x10^{13}$	0	4 600	
88	$HCO + HO_2 = CH_2O + O_2$	$1.00x10^{14}$	0	3 000	Ref. 17
89	$HCO + M = H + CO + M$	$2.94x10^{14}$	0	15 570	Ref. 20[a]
90	$HCO + O_2 = CO + HO_2$	$3.31x10^{12}$	0	7 000	Ref. 17
91	$HCO + OH = CO + H_2O$	$1.00x10^{14}$	0	0	
92	$HCO + H = CO + H_2$	$2.00x10^{14}$	0	0	
93	$HCO + O = CO + OH$	$1.00x10^{14}$	0	0	
94	$CH + O_2 = HCO + O$	$1.00x10^{13}$	0	0	Ref. 17

[a]Computed from k for the recombination reaction and the equilibrium constant expression given in Ref. 18.

TABLE I. - Concluded.

No.	Reaction	A cm^3, mole,sec	n	Ea calories	Source
95	$CO + O + M = CO_2 + M$	5.89×10^{15}	0	4 100	Ref. 17
96	$CO + O_2 = CO_2 + O$	2.51×10^{12}	0	47 690	Ref. 17
97	$CO + HO_2 = CO_2 + OH$	5.75×10^{13}	0	22 930	Ref. 17
98	$O + H_2O = OH + OH$	6.76×10^{13}	0	18 360	Ref. 17
99	$O + H_2 = OH + H$	2.95×10^{13}	0	9 800	Ref. 14
100	$H_2 + O_2 = OH + OH$	2.51×10^{12}	0	38 950	Ref. 17
101	$O + HO_2 = OH + O_2$	5.01×10^{13}	0	1 000	
102	$OH + HO_2 = H_2O + O_2$	5.01×10^{13}	0	1 000	
103	$H + HO_2 = H_2O + O$	5.01×10^{13}	0	1 000	
104	$H + HO_2 = OH + OH$	2.51×10^{14}	0	1 900	
105	$H_2 + OH = H_2O + H$	2.19×10^{13}	0	5 150	
106	$H + O_2 + M = HO_2 + M$	1.51×10^{15}	0	- 1 000	
107	$H + OH + M = H_2O + M$	1.41×10^{23}	-2	0	
108	$H + O + M = OH + M$	1.00×10^{16}	0	0	
109	$H + H + M = H_2 + M$	3.02×10^{15}	0	0	
110	$O + O + M = O_2 + M$	1.91×10^{13}	0	- 1 790	

TABLE II. - SENSITIVITY COEFFICIENTS FOR BENZENE OXIDATION IN A TURBULENT REACTOR (NITROGEN DILUTED)

[Equivalence ratio = 1.0; Initial temperature = 1115 K.]

Reaction number j	Reaction	Sensitivity coefficient of dependent variable n: $A_j/n\ (\partial n/\partial A_j)$ at time = 35 msec							
		C_6H_6	C_6H_5	C_2H_2	C_5H_6	C_6H_6OH	CO	CO_2	Temperature
1	$C_6H_6 + O_2 \rightleftharpoons C_6H_5 + HO_2$	-0.1787	-0.2050	-0.1169	0.0244	0.1129	0.0359	0.1342	0.0017
2	$C_6H_6 \rightleftharpoons C_6H_5 + H$	.8959	.0610	.5429	.3042	-.4134	.0469	-.0865	-.0004
3	$H + O_2 \rightleftharpoons OH + O$	-.0530	.2073	-.2415	.1247	-.0685	-.0025	.0196	.0001
4	$C_6H_6 + H \rightleftharpoons C_6H_6 + H_2$	.0058	.0056	.0030	-.0005	-.0027	-.0009	-.0032	-4×10^{-5}
5	$C_6H_6 + O \rightleftharpoons C_6H_5 + OH$	-.8467	-.3351	-.1150	-.2873	.1204	.0076	.2219	.0017
6	$C_6H_6 + OH \rightleftharpoons C_6H_5 + H_2O$	-.8013	-.4225	-.1949	-.3740	.1847	.0615	.0471	.0006
7	$C_6H_5 + O_2 \rightleftharpoons C_6H_5O + O$	-5.680	-6.331	-3.333	-.6433	3.089	.6679	2.870	.0349
8	$C_6H_5O \rightleftharpoons C_5H_5 + CO$	.1169	.0804	-.0435	.4413	-.1051	.0657	.2387	.0027
9	$CO + OH \rightleftharpoons CO_2 + H$	.3546	.1428	-.2367	.1347	.2001	-.1802	.6189	.0024
10	$C_5H_5 + O_2 \rightleftharpoons C_5H_5O + O$	.4904	.2212	.2088	.1859	.4070	.4003	.5624	.0110
12	$C_6H_5OH \rightleftharpoons C_6H_5O + H$	-.1854	-.0996	.3744	-.0802	.6343	-.0093	-.1608	-.0005
13	$C_5H_5 + C_6H_6 \rightleftharpoons C_5H_6 + C_6H_5$	-.1399	-.1176	-.0772	.9313	.0439	.0133	.0562	.0007
14	$OH + C_6H_6OH \rightleftharpoons C_6H_5O + H_2O$	.0065	-.0045	.1317	.0074	-.4036	.0377	-.0458	-.0003
15	$C_6H_5 \rightleftharpoons C_4H_3 + C_2H_2$	.0003	4×10^{-5}	-.0001	.0007	.0001	.0004	.0006	1×10^{-5}
17	$C_5H_6 + O \rightleftharpoons C_5H_5O + H$	.0172	.0083	.0157	-.0876	.0033	.0056	.0040	.0001
43	$C_2H_2 + O \rightleftharpoons CH_2 + CO$	.1562	.0456	-.3350	.0596	.0046	-.0038	.0050	.0001
44	$C_2H_2 + O \rightleftharpoons C_2HO + H$	.0590	.0137	-.1449	.0200	.0036	.0015	-.0080	3×10^{-5}
106	$H + O_2 + M \rightleftharpoons HO_2 + M$	-.0409	-.0039	.1975	-.0082	-.1164	.0058	-.0162	-.0002

TABLE III. - SENSITIVITY COEFFICIENTS FOR BENZENE OXIDATION IN SHOCK-HEATED ARGON

[Equivalence ratio = 1.0; initial temperature = 1405 K.]

Reaction number	Reaction	Sensitivity coefficient of dependent variable n: $A_j/n\ (\partial n/\partial A_j)$ at time = 220 μsec								
		C_6H_6	C_6H_5	C_2H_2	C_5H_6	C_6H_5OH	CO	CO_2	Temperature	Pressure
1	$C_6H_6 + O_2 \rightleftharpoons C_6H_5 + HO_2$	-0.2487	-0.0153	-0.0554	0.0781	0.3455	0.1788	0.2757	0.0042	0.0048
2	$C_6H_6 \rightleftharpoons C_6H_5 + H$	-.7186	-.1068	.0156	.3091	.3382	.6017	.8880	.0153	.0174
3	$H + O_2 \rightleftharpoons OH + O$	-.0969	-.0682	.0780	.0655	.3936	.1363	.1498	.0048	.0051
4	$C_6H_6 + H \rightleftharpoons C_6H_6 + H_2$	.0748	.0053	.0146	-.0248	-.1089	-.0554	-.0847	-.0014	-.0016
5	$C_6H_6 + O \rightleftharpoons C_6H_5 + OH$	-1.027	.1375	.1656	.0526	.7602	.4233	.6762	.0077	.0092
6	$C_6H_6 + OH \rightleftharpoons C_6H_5 + H_2O$	-.7274	.1342	-.2773	.0111	.4033	.3036	.1810	.0042	.0053
7	$C_6H_5 + O_2 \rightleftharpoons C_6H_5O + O$	-10.28	-.7590	-3.354	2.125	14.36	6.839	10.59	.1679	.1900
8	$C_6H_5O \rightleftharpoons C_5H_5 + CO$	-.2839	-.0325	.3928	.6294	.2703	.7193	.7287	-.0015	.0015
9	$CO + OH \rightleftharpoons CO_2 + H$	.0299	-.0172	.0233	.0077	.0953	-.0226	.4762	.0018	.0018
10	$C_5H_5 + O_2 \rightleftharpoons C_5H_5O + O$	-.3129	-.0680	.8683	.0440	.9106	.4974	.8584	.0204	.0220
12	$C_6H_5OH \rightleftharpoons C_6H_5O + H$	-.0048	.0030	8×10^{-5}	-.0017	.9453	-.0029	-.0020	7×10^{-5}	4×10^{-5}
13	$C_5H_5 + C_6H_6 \rightleftharpoons C_5H_6 + C_6H_5$	-.2445	.0062	-.1261	.9583	.2748	.1289	.1958	.0030	.0034
14	$OH + C_6H_6OH \rightleftharpoons C_6H_5O + H_2O$	.0005	-.0002	.0007	.0001	-.0991	.0002	-.0005	-2×10^{-6}	-2×10^{-7}
15	$C_6H_5 \rightleftharpoons C_4H_3 + C_2H_2$	-.0100	-.0148	.0889	.0116	.0956	.0449	.0700	.0017	.0018
17	$C_5H_6 + O \rightleftharpoons C_5H_5O + H$	.0030	-.0017	.0220	-.0178	.0064	.0026	.0035	.0002	.0002
43	$C_2H_2 + O \rightleftharpoons CH_2 + CO$	.0353	-.0202	-.5217	.0213	.0896	.0285	.2752	.0030	.0031
44	$C_2H_2 + O \rightleftharpoons C_2HO + H$	.0062	-.0044	-.3067	.0063	.0137	.0260	-.0854	.0009	.0009
106	$H + O_2 + M \rightleftharpoons HO_2 + M$	.0553	.0031	.0173	-.0152	-.0937	-.0388	-.0607	-.0009	-.0010

TABLE IV. - SENSITIVITY COEFFICIENTS FOR SEVERAL REACTIONS FOR TWO SHOCK IGNITIONS

Reaction number	Reaction	Sensitvity coefficient of dependent variable			
		C_6H_6	C_6H_5	CO	Pressure
(a) T_0 = 1405K φ = 1.0 Time = 220 μsec					
7	$C_6H_5 + O_2 \rightleftharpoons C_6H_5O + O$	-10.28	-0.7590	6.839	0.1900
10	$C_5H_5 + O_2 \rightleftharpoons C_5H_5O + O$	-.3129	-.0680	.4974	.0220
8	$C_6H_5O \rightleftharpoons C_5H_5 + CO$	-.2839	-.0325	.7193	.0015
6	$C_6H_6 + OH \rightleftharpoons C_6H_5 + H_2O$	-.7274	.1342	.3036	.0053
15	$C_6H_5 \rightleftharpoons C_4H_3 + C_2H_2$	-.0100	-.0148	.0449	.0018
(b) T_0 = 1600K φ = 2.0 Time = 140 μsec					
7	$C_6H_5 + O_2 \rightleftharpoons C_6H_5O + O$	-2.057	-1.208	2.663	0.1927
10	$C_5H_5 + O_2 \rightleftharpoons C_5H_5O + O$	-.1582	-.1595	.4286	.0399
8	$C_6H_5O \rightleftharpoons C_5H_5 + CO$	-.0393	-.0122	.0938	.0036
6	$C_6H_6 + OH \rightleftharpoons C_6H_5 + H_2O$	-.3172	.1390	.2488	.0150
15	$C_6H_5 \rightleftharpoons C_4H_3 + C_2H_2$	-.2875	-.6623	1.040	.0930

TABLE V. - SENSITVITY OF COMPUTED IGNITION DELAY TIME TO RATE CONSTANT VARIATION FOR TWO SHOCK IGNTIIONS

Reaction number	Reaction	τ_p, μs k_{std}	τ_p, μs 2 k_{std}	Percent change	τ_p, μs 0.5 k_{std}	Percent change
(a) T_0 = 1405K, φ = 1.0						
7	$C_6H_5 + O_2 \rightleftharpoons C_6H_5O + O$	272	188	-30.9	420	54.4
10	$C_5H_5 + O_2 \rightleftharpoons C_5H_5O + O$		246	-9.6	313	15.1
8	$C_6H_5O \rightleftharpoons C_5H_5 + CO$		268	-1.5	289	6.3
6	$C_6H_6 + OH \rightleftharpoons C_6H_5 + H_2O$		273	.4	280	2.9
15	$C_6H_5 \rightleftharpoons C_4H_3 + C_2H_2$		272	0	276	1.5
(b) T_0 = 1600K, φ = 2.0						
7	$C_6H_5 + O_2 \rightleftharpoons C_6H_5O + O$	151	108	-28.5	203	34.4
10	$C_5H_5 + O_2 \rightleftharpoons C_5H_5O + O$		143	-5.3	160	6.0
8	$C_6H_5O \rightleftharpoons C_5H_5 + CO$		151	0	154	2.0
6	$C_6H_6 + OH \rightleftharpoons C_6H_5 + H_2O$		149	-1.3	159	5.3
15	$C_6H_5 \rightleftharpoons C_4H_3 + C_2H_2$		125	-17.2	172	13.9

TABLE VI. - BENZENE-OXYGEN-ARGON INITIAL CONDITIONS

Mixture number	Equivalence ratio, Φ	Mole percent			Initial temperature range, (behind reflected shock), K
		C_6H_6	O_2	Ar	
1	0.5	1.354	20.313	78.333	1209-1345
2	1.0	.516	3.868	95.616	1345-1528
3	1.0	1.69	12.68	85.63	1283-1435
4	1.0	1.69	12.582	85.728	1355-1408
5	2.0	1.354	5.093	93.555	1363-1600

TABLE VII. - COMPARISON OF COMPUTED AND EXPERIMENTAL IGNITION DELAYS

Equivalence ratio φ	Percent argon	Initial temperature K	Experimental ignition delay, μsec	Computed ignition delay, μsec	Percent difference	Standard deviation percent
0.5	78.3	1209	878	680	-22.6	52.5
		1227	743	600	-19.2	
		1254	435	498	14.5	
		1276	330	431	30.6	
		1291	272	388	42.6	
		1307	185	352	90.3	
		1314	202	334	65.3	
		1345	159	280	76.1	
1.0 Dilute	95.6	1345	755	550	-27.1	22.0
		1374	604	450	-25.5	
		1402	415	370	-10.8	
		1412	412	345	-16.3	
		1428	367	313	-14.7	
		1482	213	216	1.4	
		1525	122	160	31.1	
		1528	122	159	30.3	
1.0 Strong	85.6	1283	750	600	-20.0	28.3
		1290	613	575	-6.2	
		1294	607	556	-8.4	
		1328	490	450	-8.2	
		1355	303	378	24.7	
		1369	287	342	19.2	
		1379	291	320	10.0	
		1405	198	272	37.4	
		1408	189	266	40.7	
		1417	178	252	41.6	
		1435	151	225	49.0	
2.0	93.6	1363	1520	870	-42.8	21.6
		1415	890	607	-31.8	
		1457	599	453	-24.4	
		1540	274	248	-9.5	
		1554	243	223	-8.2	
		1570	211	195	-7.6	
		1582	157	172	9.6	
		1600	154	151	-1.9	

Standard deviation of all data points is 33.2 percent.

TABLE VIII. - COMPUTED AND EXPERIMENTAL ACTIVATION ENERGIES FOR IGNITION DELAY

Equivalence ratio φ	Activation energy cal/mole		Percent difference
	Experimental	Computed	
0.5	44160	21230	-52
1.0 Dilute	41470	27860	-37
1.0 Strong	37250	23560	-37
2.0	42400	32010	-24

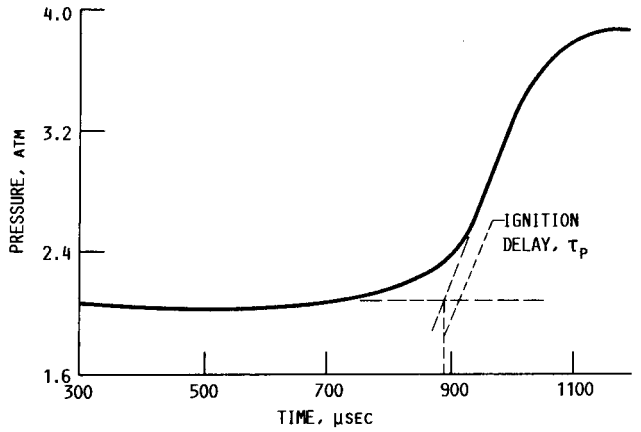

FIGURE 1. - COMPUTED PRESSURE AS FUNCTION OF TIME FOR BENZENE-OXYGEN-ARGON SHOCK IGNITION. INITIAL TEMPERATURE, 1363 K; EQUIVALENCE RATIO, φ, 2.0.

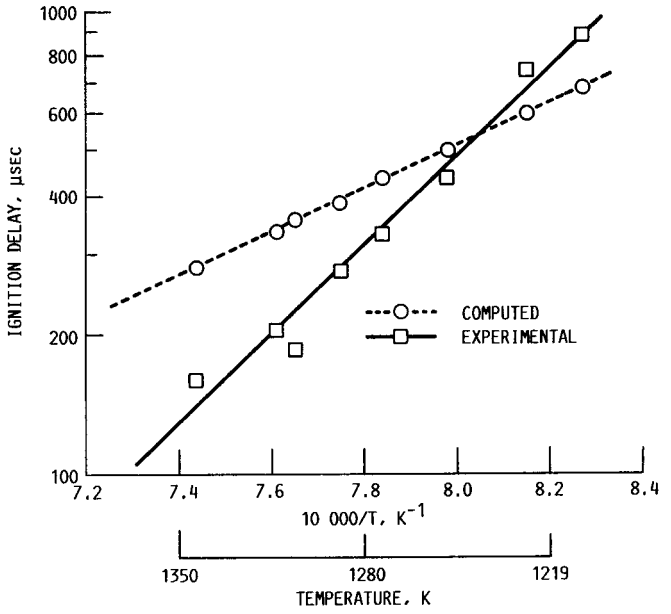

FIGURE 2. - BENZENE-OXYGEN-ARGON IGNITION DELAY VERSUS RECIPROCAL OF TEMPERATURE FOR EQUIVALENCE RATIO 0.5.

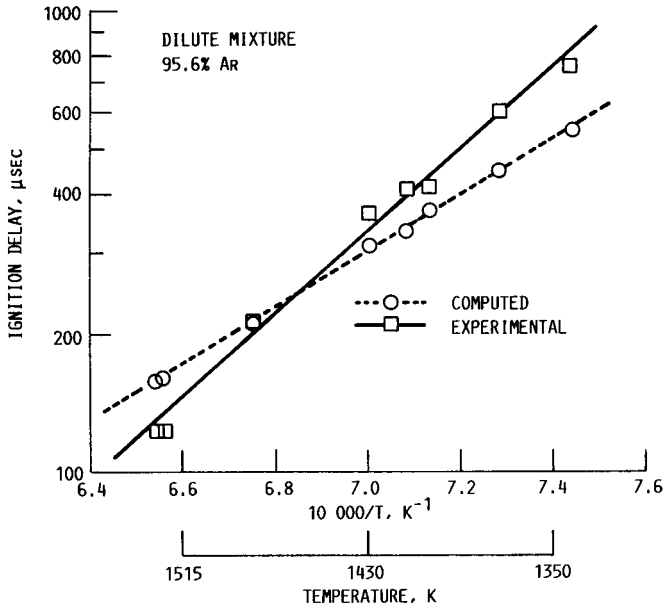

FIGURE 3. - BENZENE-OXYGEN-ARGON IGNITION DELAY VERSUS RECIPROCAL OF TEMPERATURE FOR EQUIVALENCE RATIO 1.0.

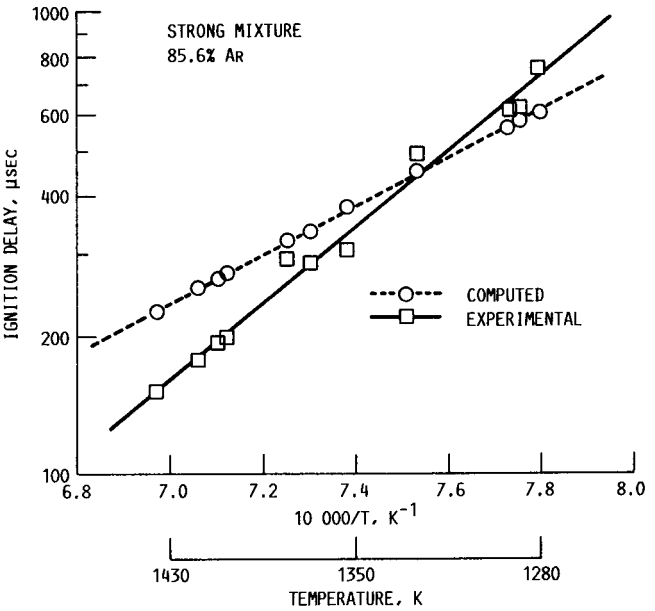

FIGURE 4.- BENZENE-OXYGEN-ARGON IGNITION DELAY VERSUS RECIPROCAL OF TEMPERATURE FOR EQUIVALENCE RATIO 1.0.

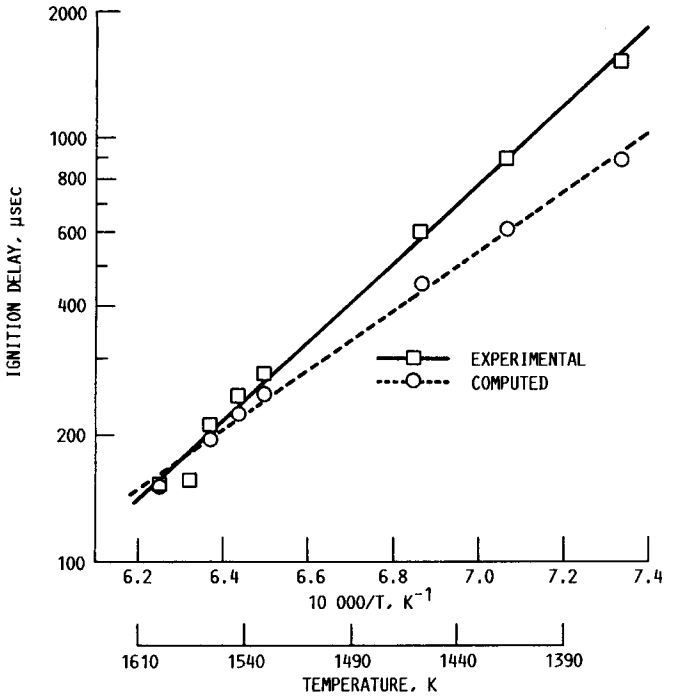

FIGURE 5. - BENZENE-OXYGEN-ARGON IGNITION DELAY VERSUS RECIPROCAL OF TEMPERATURE FOR EQUIVALENCE RATIO 2.0.

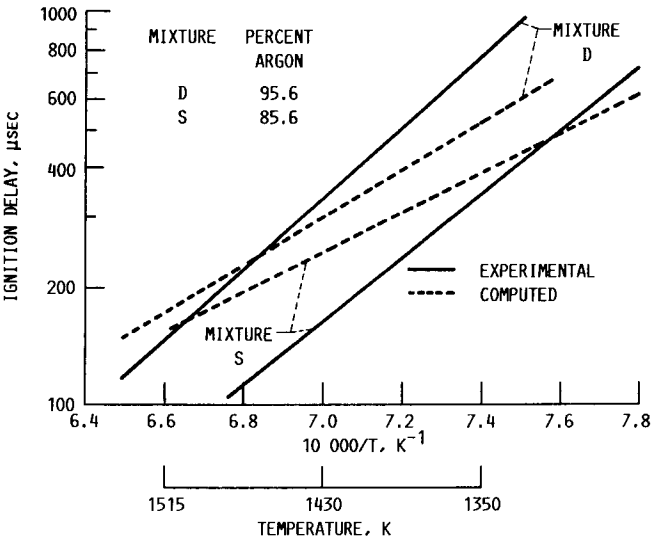

FIGURE 6. - BENZENE-OXYGEN-ARGON IGNITION DELAY VERSUS RECIPROCAL OF TEMPERATURE: EFFECT OF ARGON DILUTION FOR EQUIVALANCE RATIO 1.0.

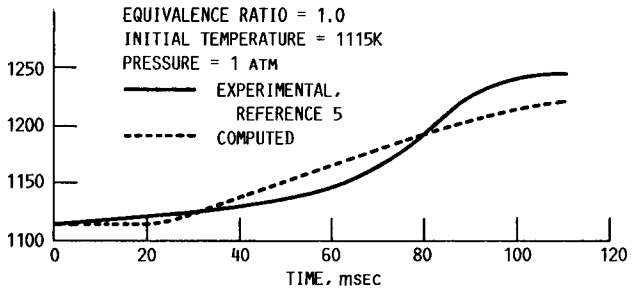

FIGURE 7. - TEMPERATURE VERSUS TIME FOR BENZENE-OXYGEN-NITROGEN REACTION.

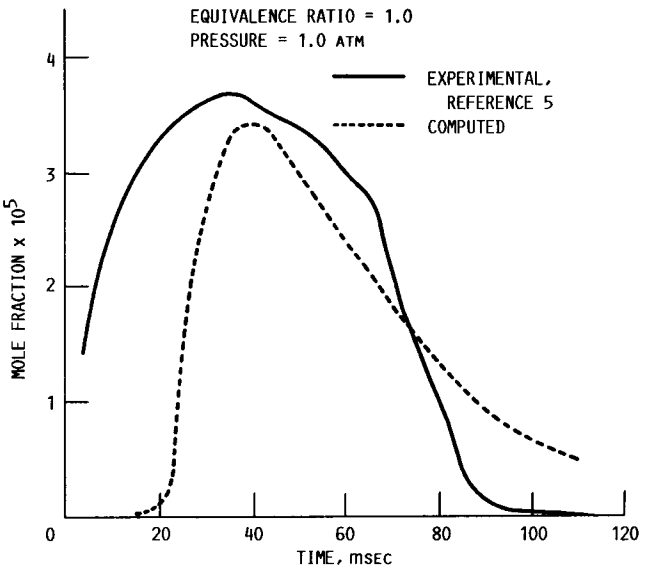

FIGURE 8. - CYCLOPENTADIENE MOLE FRACTION VERSUS TIME FOR BENZENE-OXYGEN-NITROGEN REACTION.

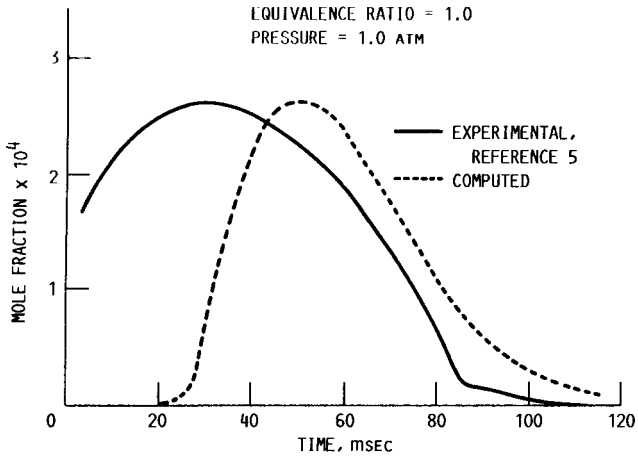

FIGURE 9. - PHENOL MOLE FRACTION VERSUS TIME FOR BENZENE-OXYGEN-NITROGEN REACTION.

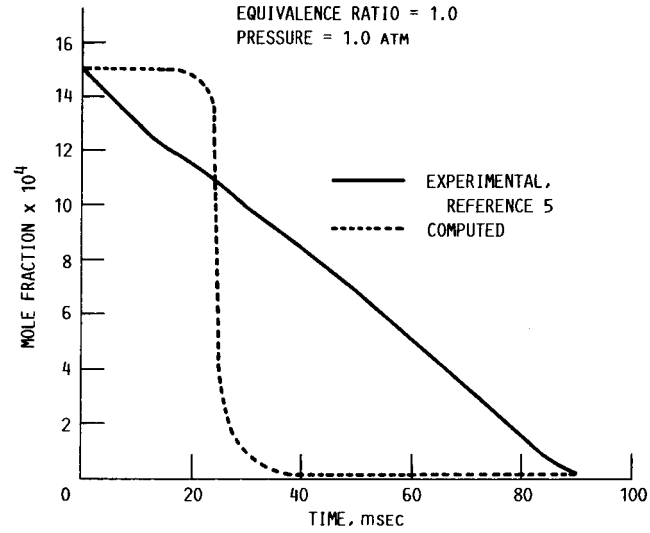

FIGURE 10. - BENZENE MOLE FRACTION VERSUS TIME FOR BENZENE-OXYGEN-NITROGEN REACTION.

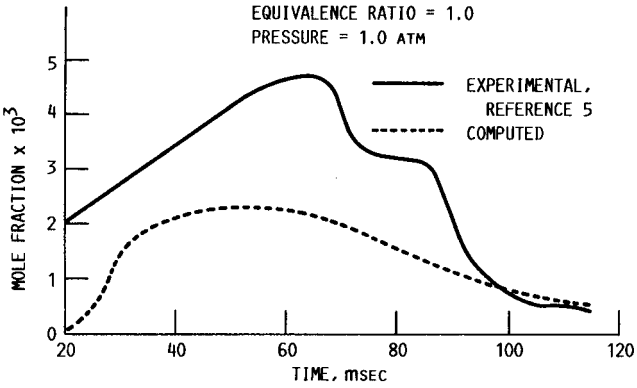

FIGURE 11. - CARBON MONOXIDE MOLE FRACTION VERSUS TIME FOR BENZENE-OXYGEN-NITROGEN REACTION.

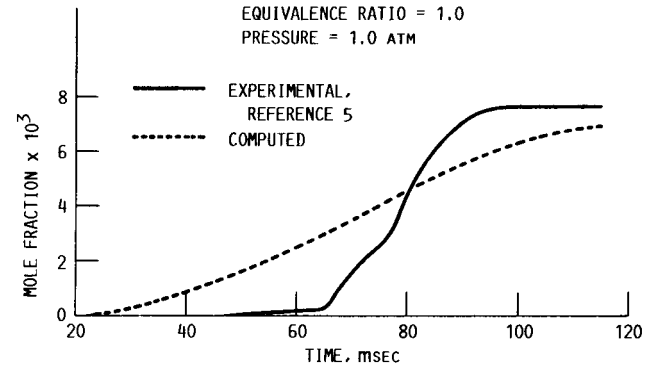

FIGURE 12. - CARBON DIOXIDE MOLE FRACTION VERSUS TIME FOR BENZENE-OXYGEN-NITROGEN REACTION.

NASA
National Aeronautics and Space Administration

Report Documentation Page

1. Report No.	2. Government Accession No.	3. Recipient's Catalog No.
NASA TM-100202		

4. Title and Subtitle	5. Report Date
Detailed Mechanism of Benzene Oxidation	October 1987
	6. Performing Organization Code

7. Author(s)	8. Performing Organization Report No.
David A. Bittker	E-3797
	10. Work Unit No. 505-62-21

9. Performing Organization Name and Address	11. Contract or Grant No.
National Aeronautics and Space Administration Lewis Research Center Cleveland, Ohio 44135-3191	
	13. Type of Report and Period Covered: Technical Memorandum
12. Sponsoring Agency Name and Address	14. Sponsoring Agency Code
National Aeronautics and Space Administration Washington, D.C. 20546-0001	

15. Supplementary Notes

16. Abstract

A detailed quantitative mechanism for the oxidation of benzene in both argon and nitrogen diluted systems is presented. Computed ignition-delay times for argon-diluted mxitures are in satisfactory agreement with experimental results for a wide range of initial conditions. An experimental temperature versus time profile for a nitrogen-diluted oxidation has been accurately matched and several concentration profiles have been matched qualitatively. Application of sensitivity analysis has given approximate rate constant expressions for the two dominant heat-release reactions, the oxidations of C_6H_5 and C_5H_5 radicals by molecular oxygen.

17. Key Words (Suggested by Author(s))	18. Distribution Statement
Benzene oxidation Chemical mechanisms Ignition delay times	Unclassified - Unlimited Subject Category 25

19. Security Classif. (of this report)	20. Security Classif. (of this page)	21. No of pages	22. Price*
Unclassified	Unclassified	23	A02

NASA FORM 1626 OCT 86

*For sale by the National Technical Information Service, Springfield, Virginia 22161